

Design and Analyse of Silicon Carbide JFET Based Inverter

Zheng Xu¹, Sanbo Pan²

¹School of Electrical and Electronic Engineering, East China Jiaotong University
Nanchang, China, 330013

187391733@qq.com

² Department of Electrical engineering, Anyang Normal University
Eastern Yellow River Ave, Anyang, Henan, China, 455000
pansan@aynu.edu.cn

Abstract: - This paper presents the design and testing of a high frequency, high efficiency inverter using silicon carbide (SiC) JFET power module. A rugged negative voltage gate drive circuit is used to solve the normally on problem of JFET devices and avoid the bridge shot-through during power on or power off. The circuit can provide over-voltage protection, over current protection and over temperature protection circuits to ensure the safe operation of the SiC JFET module and the resultant inverter system. The simulation and measurement results show that SiC JFETs have short turn-on and turn-off times, which will result in lower switching losses than silicon (Si) IGBTs. The low on-resistance in SiC JFETs will result in lower conduction losses. The experiment results of a 1kW SiC JFET-based inverter showed 3% efficiency improvement by a SiC JFET-based inverter over a Si IGBT-based inverter.

Key-Words: - Silicon Carbide, SiC JFET, inverter, gate drive

1 Introduction

For several decades silicon (Si) has been the preferred material for nearly all semiconductors. Processing of silicon has become very mature and cost efficient. Research on alternative materials is about as old as the application of silicon. In particular so called wide bandgap semiconductors, like gallium nitride GaN and silicon carbide SiC, have very interesting characteristics. In [1], the author indicted the factors of several power semiconductor materials, it shows other wide gap materials have better performance than Si materials in power semiconductor application.

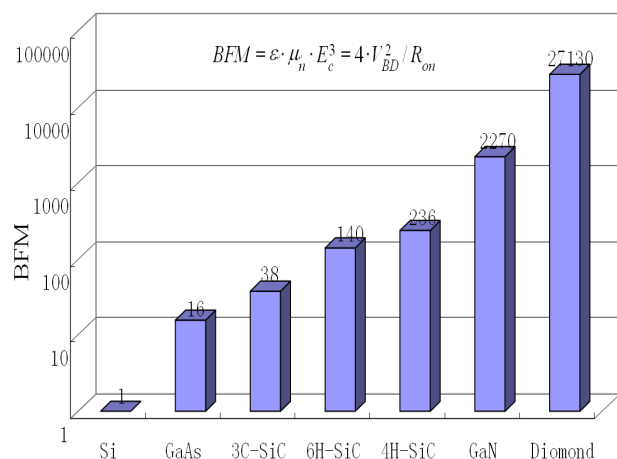


Fig. 1 Performance factor compare of semiconductor materials

For high performance power semiconductors SiC is the preferred choice. Silicon carbide (SiC) semiconductor has the characteristics of wide bandgap (3.0eV for 6H-SiC), higher saturation velocity (2×10^7 cm/s), high thermal conductivity (3.3-4.9 W/cmK), low on resistance ($1 \text{ m}\Omega/\text{cm}^2$) and high breakdown electric field strength (2.4MV/cm) [1-16]. Therefore, SiC power devices will have the advantages of larger current carrying capability, higher voltage block capability, high operating temperature, and less static and dynamic losses than traditional silicon (Si) power switches. In addition, SiC power devices can operate at higher switching frequencies. Therefore, in a inverter system using SiC power devices, the size of its passive components (inductor and capacitor) can be reduced due to the higher frequency operation, so does the associated heatsinks due to lower losses generated as compared with a conventional Si system. At the present time, it is still difficult to produce SiC MOSFET. SiC JFET, on the other hand, is easier to be manufactured and currently is at engineering stage that is being commercialized. As the manufacture technique improves and its mass production can be realized, it is anticipated that

there will be more SiC JFET power switches used in power electronic systems.

SiC JFETs are “normally-on” devices. For SiC JFETs to be incorporated in the presently used power converter system designs[17-20], there are two possible solutions. One is to use negative voltage to turn it off. For example [17], a flyback transformer was used to generate the negative gate drive voltage to turn off the SiC JFET. This technique is suitable for DC/DC converters with narrow variation of duty cycle. The other solution is to use a SiC JFET plus a low on-resistance Si MOSFET cascade to form a normally off controlled SiC switch [21-22]. In this design, the gating circuit same as conventional MOSFETs can be used in the inverter applications like normal MOSFETs. However, the introduction of the additional Si MOSFET will add the system cost and bring additional losses.

This paper presents the development of a high-frequency, high-efficiency inverter using SiC JFET modules. In this system, a negative gate drive voltage is used to turn off the SiC JFET, and the gate driver circuit gets power from the DC rail to ensure the safe operation of SiC JFET devices. In addition, the gate driver circuit is optical-isolated and the control logic is the same as traditionally normally off devices. This design enables the integration of the SiC JFET, the driver circuit and the protect circuit into one smart power module. The simulation and experiment results of a SiC JFET inverter and an IGBT inverter demonstrated the low on-state voltage drop and high switching speed prospects of SiC power JFET. The SiC JFET Module inverter using a SiC JFET module shows more than 3% higher efficiency than the new-generation Si IGBT based inverter in wide switching frequency ranges.

2 Circuits Design

This paper designed a three phase SiC JFET module based inverter, it include the main circuit, voltage, current and temperature sensing circuit, PWM and protection circuit, power and drive circuit. The design of this SiC JFET inverter is shown in Fig. 2. When DC power input, through soft start circuit, and EMI filter, it flow through a SiC JFET module based three phase inverter, get the AC power. The inverter also include power supply circuit, digital SVPWM signal generator circuit, protection circuit and drive circuit.

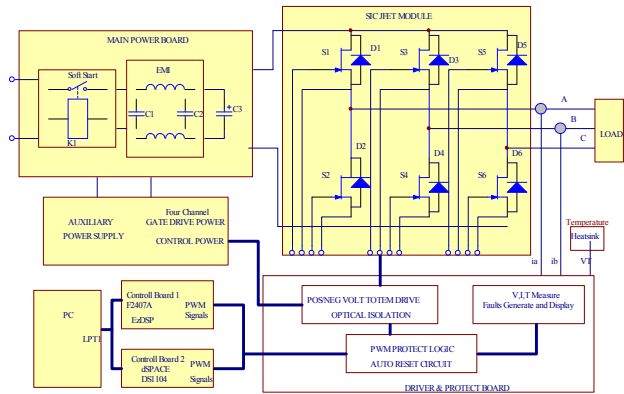


Fig. 2 SiC-JFET based inverter system

2.1 Main circuit design

The main circuit is similar to a traditional inverter circuit, shown in Fig. 3. Which consists of the soft start relay, EMI filter, bulk capacitor, SiC JFET module (six packed SiC JFET and anti-parallel SiC diode).

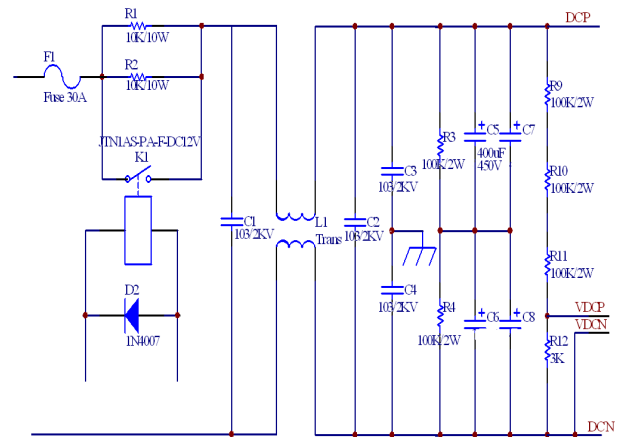


Fig. 3 SiC-JFET based inverter main circuit

2.2 Sense circuit design

The sense circuit include the DC input voltage sensing, AC output voltage sensing and heatsink temperature sensing. These sensed signal can prevent the SiC JFET module damaged by over voltage, over current or over temperature situation.

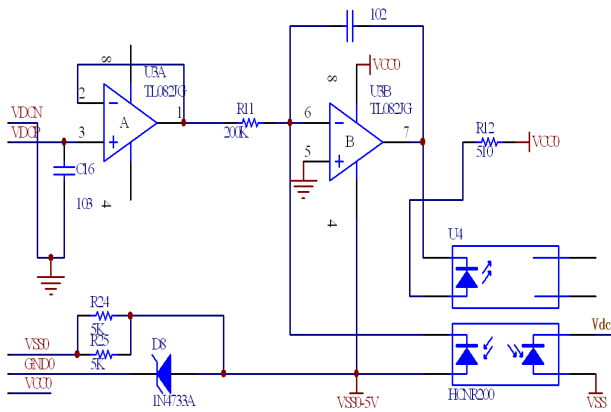


Fig. 4 DC voltage sense circuit

DC voltage sense circuit using the high precision linear optocoupler to get the value of high input voltage, shown in Fig.4.

AC current sense circuit using the high precision current Hall sensor to get the precision value of current and get a quick response, shown in Fig.5.

Temperature sensor, the LM35, is a precision integrated-circuit temperature sensor, whose output voltage is linearly proportional to the Centigrade temperature. It has 0.5 degree accuracy guarantee.

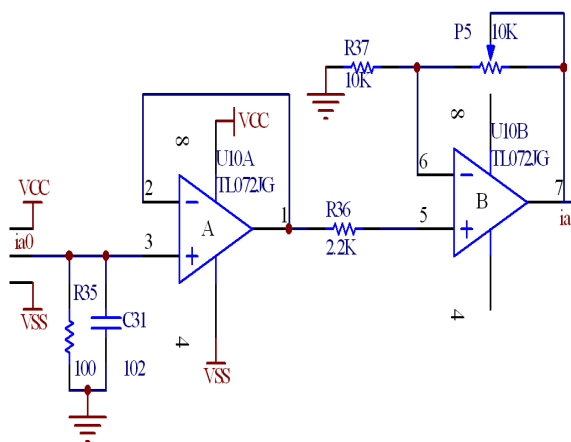


Fig. 5 AC current sense circuit

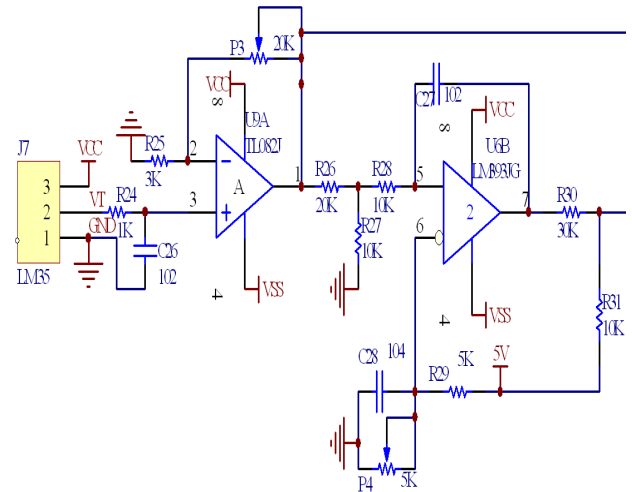


Fig. 6 Temperature sense circuit

2.3 Protection circuit design

The protection circuit includes three-phase over current protection, DC bus over voltage protection and over temperature protection. It also has the bridge drive signal short-through lock to prevent the SiC JFETs short through damage. All the protection signals combined one FAULT signal in Fig.7.

The PWM signals are generated from DSP TMS320F2407 or dSPACE DS1104 system. There is a TTL and CMOS voltage compatible problem, the PWM signals from DSP are TTL voltage standard, but other protection signals, such as FAULT is CMOS voltage standard, so use the logic IC which is compatible to both of TTL and CMOS voltage standard. Then the output signals is sent to driver board to gate the SiC JFET module. The protection circuit also include fault LED display and auto reset circuit according to each protection circuit.

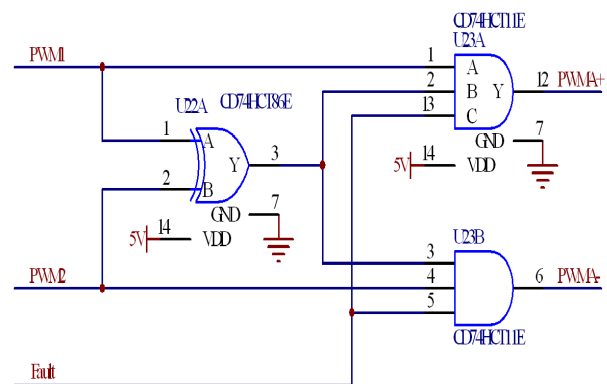


Fig. 7 Bridge drive signals short-through protection circuit

2.4 Drive circuit design

For the SiC-JFET-Module-based inverter system, one important and special issue is the gate drive circuit design. Because of the “normally on” feature of SiC JFET, the SiC JFET turns on at gate voltage close to 0V. A negative voltage, usually -24V, is necessary to turn off the SiC JFET.

The negative gate drive voltage must block the module to prevent the shot-through of the bridge when system is powered up. This implies that negative gate voltage must be applied before the DC-rail voltage is applied to the SiC JFETs. In addition, the negative gate voltage should also force the SiC JFET devices off when the inverter is powered off and the discharge of bulk capacitor is not initiated yet.

The gating logic in Fig. 9 is similar to that of a conventional inverter. When the PWM signal from the digital controller is high, then the gating voltage is equal to VCC(5V) and the SiC JFET turns on. When PWM signal from the digital controller is low, then the gating voltage is equal to VSS (-24), and the SiC JFET turns off.

In this paper, the DC rail voltage is used to power the driver circuit as shown in Fig. 8. This design can avoid the unexpected breakthrough of SiC JFETs. At startup, the DC rail voltage is applied to the gate drive circuit before the startup relay closes. The relay only closes once the negative gate voltage is generated and applied to the gates of SiC JFETs. The gate driver circuit is designed to be optical-isolated, so that it is convenient to integrate this driver circuit later into the power module, and make

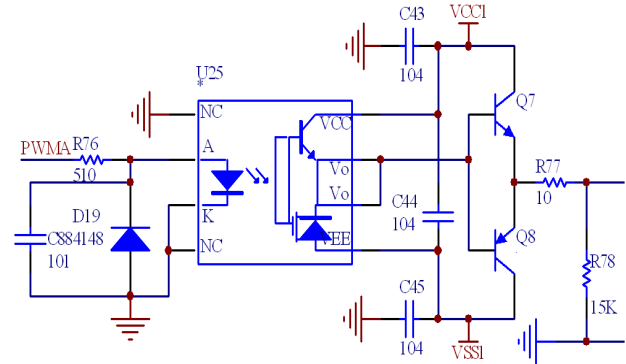


Fig. 9 SiC JFET gate drive circuit

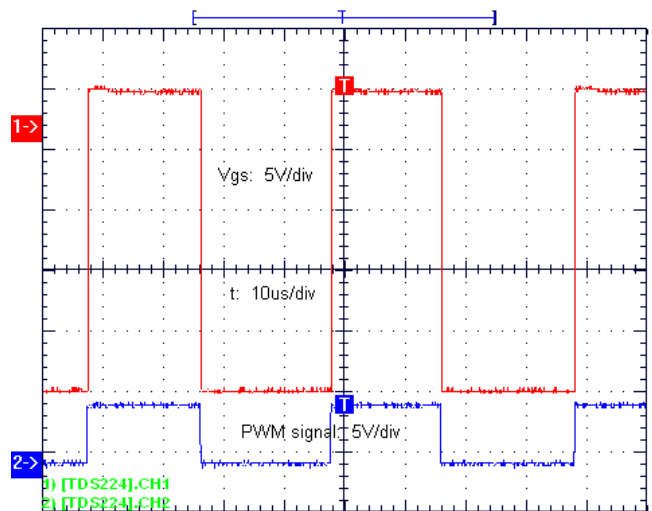


Fig. 10 Drive signal waveforms

the application of SiC JFET more feasible with the normally-on issue. Fig. 10 shows the measured PWM waveform from the digital controller, and the gate drive circuit.

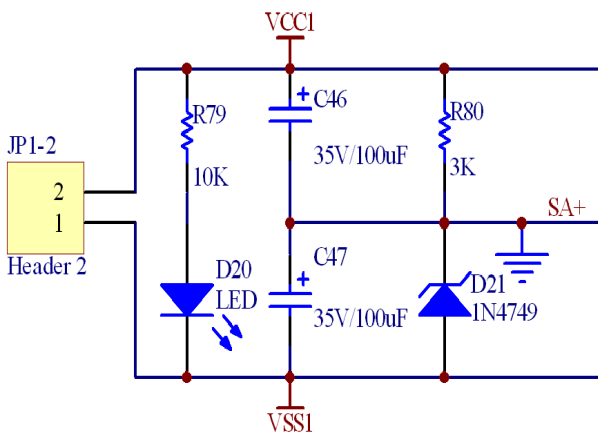


Fig. 8 Drive circuit power supply

3 Simulation and Loss Analysis

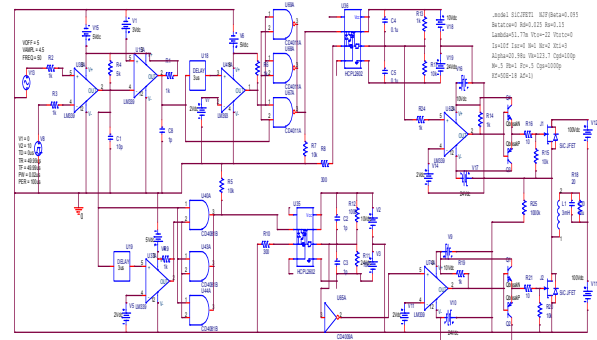


Fig. 11 SiC JFET inverter simulation circuit

Before the experiment, a Pspice model of SiC JFET and SiC JFET-based circuit was established as shown in Fig. 11. Simulation parameters are from

SiC JFET die manufacturing company and test results [9] [23-24]. Each die has a maximum drain-source voltage great than 1200V (@Q25°C, Idss<2mA), maximum drain-source leakage current less than 0.4 mA (@Q25°C, 400 V), 7 amperes rated drain- source current, and Ron < 0.25 Ohm (@25°C). There are 2 to 4 dies parallel to form one switch unit.

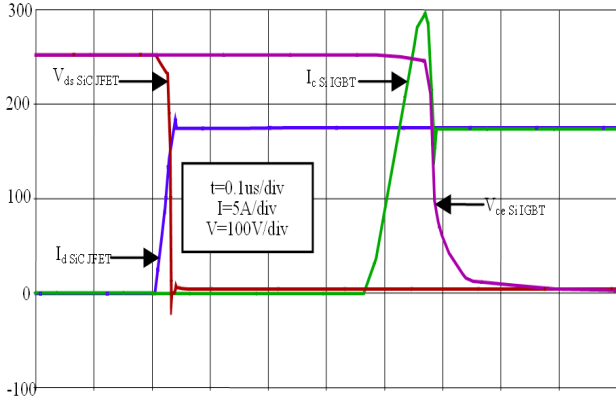


Fig. 12 Turn-on waveforms SiC JFET vs. IGBT

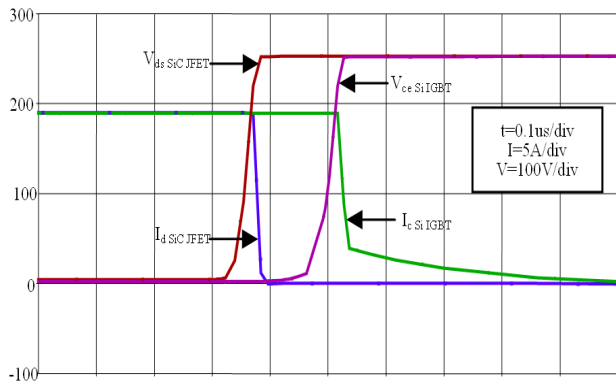


Fig. 13 Turn-off waveforms SiC JFET vs. IGBT

Fig. 12 and Fig. 13 show the simulated turn on and turn off waveforms of Si IGBT and SiC JFET. The turn-on time of the SiC JFET is about 50ns while the turn-on time of IGBT is about 100ns. The turn-off time of the SiC JFET is about 50ns while the one of IGBT is about 100ns with a 0.5us tail current time.

To calculate the losses of the SiC JFET inverter with sinusoidal output, assume the sinusoidal current lagging the sinusoidal output voltage an angle of θ , as shown in Fig. 14.

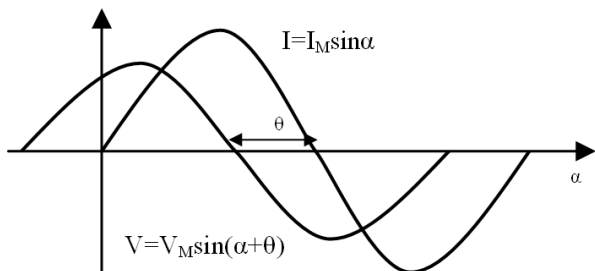


Fig. 14 V/I waveforms of the inverter output

The angle corresponds to a constant power factor. Similar to the loss calculation of conventional hard switching inverter [25-27], the conduction and switching losses of the SiC JFET and SiC diode can be derived as following.

3.1 Conduction Loss

For large ratio between carrier frequency and modulation frequency, the duty cycle of the power switch and anti-parallel diode function are:

$$\begin{cases} D_s(\alpha) = \frac{1}{2} [1 + m \sin(\alpha + \theta)] \\ D_d(\alpha) = \frac{1}{2} [1 - m \sin(\alpha + \theta)] \end{cases} \quad (1)$$

α is the phase angle of current waveform and m is modulation index. The power switch and diode conduction loss within any angle α is:

$$\begin{cases} P_s(\alpha) = [I_M \sin(\alpha) \cdot V_{s(on)}(I) \cdot D_s(\alpha)] \\ P_d(\alpha) = [I_M \sin(\alpha) \cdot V_{d(on)}(I) \cdot D_d(\alpha)] \end{cases} \quad (2)$$

Where

$$\begin{cases} V_{s(on)}(I) \approx I_M \sin(\alpha) \cdot R_{s(on)} \\ V_{d(on)}(I) \approx V_f + I_M \sin(\alpha) \cdot R_{d(on)} \end{cases} \quad (3)$$

Each device's averaged conduction time is only one half of the switching period, so

$$P_{avg} = \frac{1}{2\pi} \int_0^\pi P(\alpha) d\alpha \quad (4)$$

Therefore the conduction loss of SiC JFET and the SiC diode can be obtained

$$\begin{cases} P_{s(con)} = \left[(I_M)^2 \cdot R_{s(on)} \cdot \left(\frac{\sqrt{3}}{8\sqrt{\pi}} + \frac{m}{3\pi} \cos \theta \right) \right] \\ P_{d(con)} = \frac{1}{2} I_M \cdot V_f \left(\frac{1}{\pi} - \frac{m}{4} \cos \theta \right) + (I_M)^2 \cdot R_{d(on)} \cdot \left(\frac{\sqrt{3}}{8\sqrt{\pi}} - \frac{m}{3\pi} \cos \theta \right) \end{cases} \quad (5)$$

3.2 Switching Loss

To calculate the switching loss, the current and voltage are assumed to vary lineally during the switching on and off as shown in Fig. 15. Because the SiC diode has nearly no reverse recovery current, the switch has no turn-on loss caused by diode reverse current and has no reverse recovery loss. From Fig. 15, the turn-off loss is

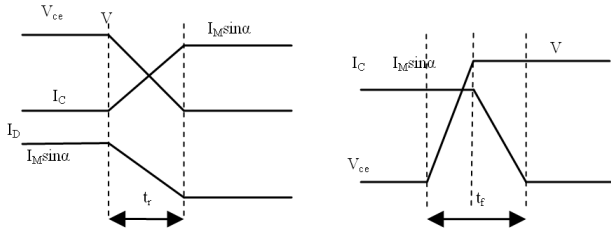


Fig. 15 Vce and Ic waveform during switching

$$E_{off} = V \cdot I_o \cdot t_{off} / 2 \quad (6)$$

The average turn-off loss in the whole period is

$$P_{off} = f_s \cdot \frac{1}{\pi} \int_0^\pi E_{off} \cdot d\alpha = \frac{V \cdot I_M \cdot t_{off} \cdot f_s}{\pi} \quad (7)$$

Similarly, the turn-on loss is

$$E_{on} = V \cdot I_o \cdot t_{on} / 6 \quad (8)$$

The average switching on losses in one period is

$$P_{on} = f_s \cdot \frac{1}{\pi} \int_0^\pi E_{on} \cdot d\alpha = \frac{V \cdot I_M \cdot t_{on} \cdot f_s}{3\pi} \quad (9)$$

For the 1kW inverter, the calculated loss and efficiency curve of SiC JFET module and the 3rd generation Si IGBT module are shown in Table I. The SiC JFET is a full bridge one, each switch unit is composed by two SiC JFET and a antiparallel SiC Schottky diode, the 3rd generation Si IGBT module using the up to date stg3p3m25n60 from ST company. Because the SiC has very low on-resistance, and short switch on/off time, the conduction loss and switching losses of SiC JFET are much lower than that of Si IGBT.

By adding losses of other circuit components (driving circuit, relay, power supply, etc.), the efficiency of SiC JFET inverter and Si IGBT inverter at different switching frequency can be calculated, as shown in Fig. 16. It can be seen that the SiC JFET inverter has much higher efficiency than Si IGBT inverters and is more suited for high frequency applications.

TABLE I. Calculated losses of SiC-JFET module v.s. 3rd generation Si-IGBT module @ VDC=200V, P=1kw (W)

	20kHz		50kHz		100kHz	
	SiC JFET	Si IGBT	SiC JFET	Si IGBT	SiC JFET	Si IGBT
P _{Scond}	2.1	10.5	2.1	10.5	2.1	10.5
P _{Dcond}	1.3	7.3	1.3	7.3	1.3	7.3
P _{S on}	0.5	1.2	1.25	3	2.5	6
P _{S off}	3.1	10.1	7.7	25.25	15.5	50.5
P _{D reverse}	0	2.2	0	5.5	0	11

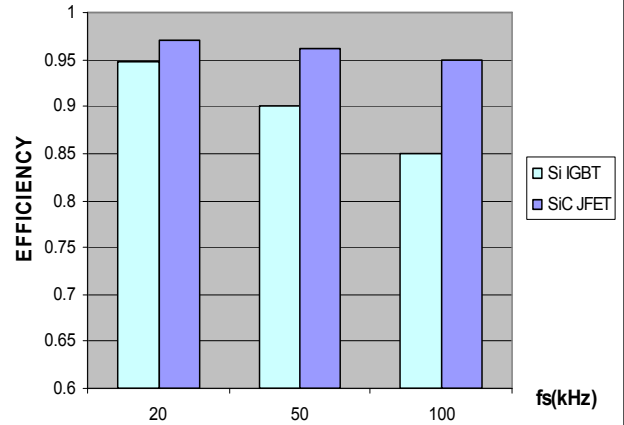


Fig. 16 Calculated efficiency of SiC JFET module vs Si IGBT module

4 Experiment Results

The 1kW, 200V inverter was built in Fig.17. Fig. 18 shows the inverter circuit prototype and tested with both Si IGBT and SiC JFET as shown in Fig. 19. Test results of the three-phase inverter prototype using SiC JFET (with anti-parallel SiC diode) validated the simulation and calculations.

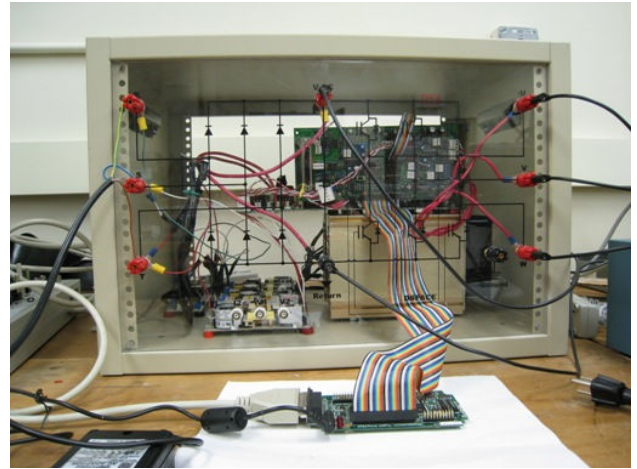


Fig. 17 Whole inverter prototype assembly

The circuit for measuring the switching on/off times is show in Fig. 19, and the inverter measurement circuit is show in Fig. 20. Yokogawa PZ4000 power analyzer is used to record and analyze the efficiency and output current quality of the inverter. The load connected to the inverter is a three-phase induction machine rated at 3 Hp, 60Hz, 1800 rpm, 208V, and 10.8A.

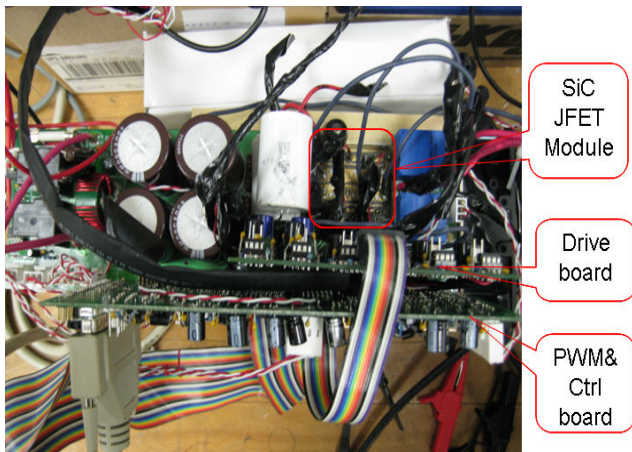


Fig. 18 SiC module based inverter circuits

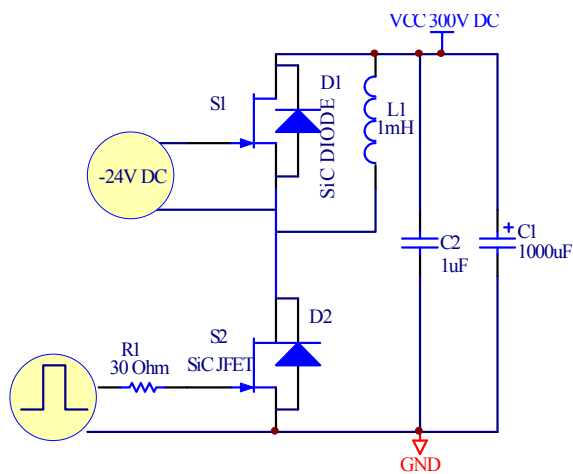


Fig. 19 Circuit measuring switching times

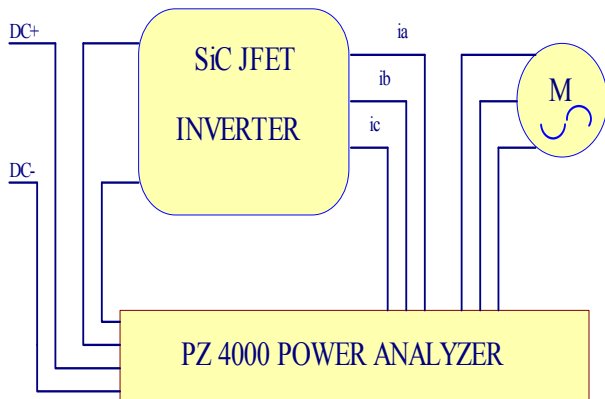


Fig. 20 Circuit for measuring inverter efficiency

Fig.21 shows the compare of forward and reverse on resistance characteristics of SiC JFET. Fig.22 shows the Forward voltage drop of SiC parasitic diode and antiparallel Schottky diode. Fig.23 shows the block voltage V_{ds} vs. V_{gs} of SiC JFET.

Fig. 24 shows the experimental V_d and I_d turn on waveforms of the Si IGBT. Fig. 25 shows the experimental V_d and I_d turn on waveforms of the SiC JFET. Fig. 26 shows the experimental V_d and

I_d turn off waveforms of the Si IGBT. Fig. 27 shows the V_d and I_d turn off waveforms of the SiC JFET.

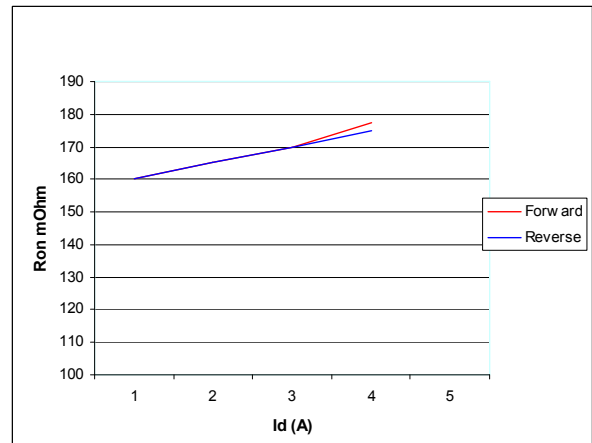


Fig. 21 On resistance of SiC JFET

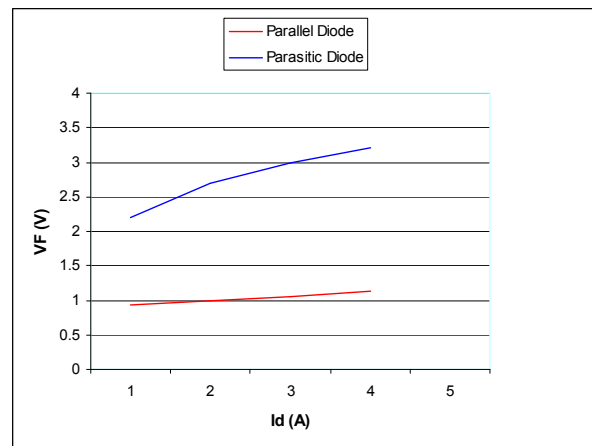


Fig. 22 Forward voltage drop of SiC Schottky diode

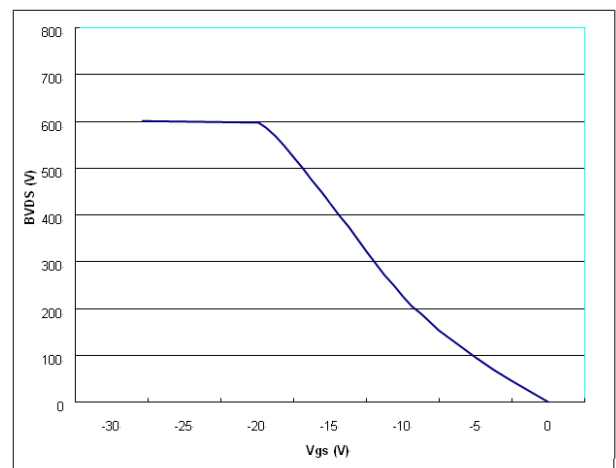


Fig. 23 Block voltage V_{ds} vs. V_{gs} of SiC JFET

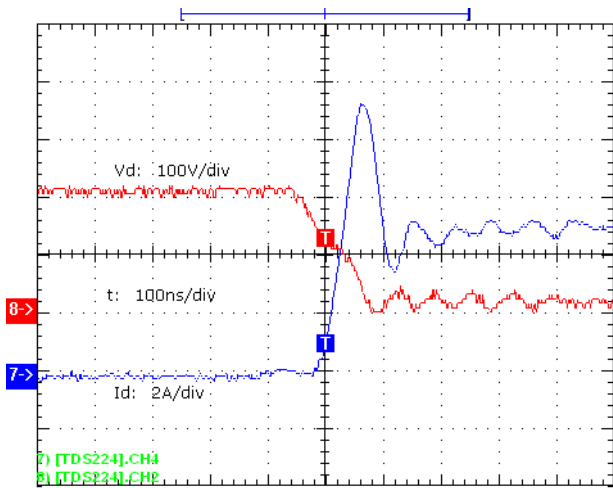


Fig. 24 IGBT module turn-on waveforms

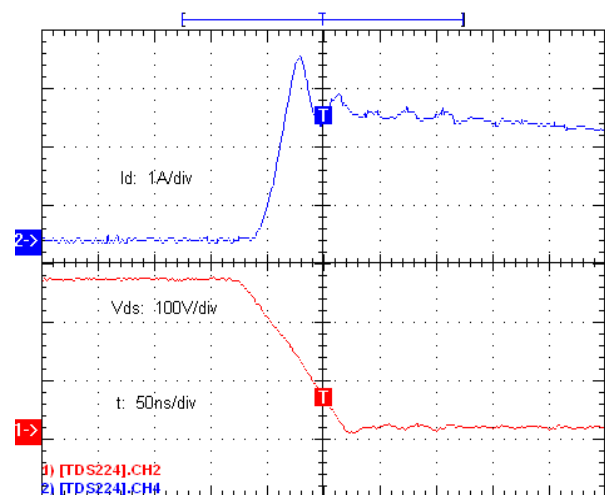


Fig. 25 SiC JFET module turn-on waveforms

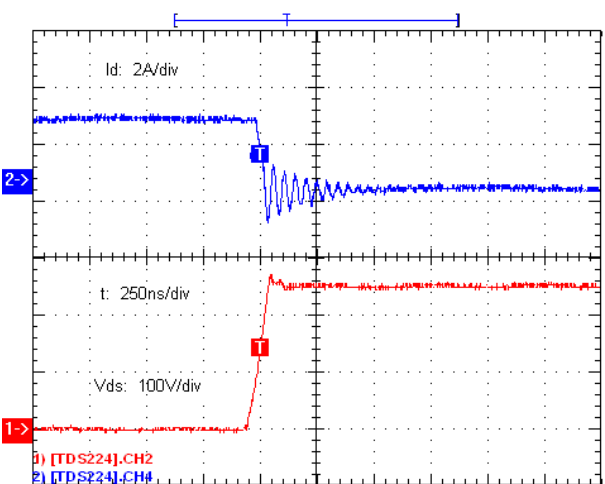


Fig. 26 IGBT module turn-off waveforms

Fig. 28 shows the experimental reverse recovery current I_{rr} waveforms of the Si IGBT. Fig. 29 shows the experimental reverse recovery current I_{rr} waveforms of SiC JFET. The tested turn-on time of SiC module is approximately 80ns and turn off time is approximately 100ns. The turn-on time is mainly

attributed by the test circuit parameters [28]. For the purpose of comparison, Si IGBT module use similar gating circuitry as of SiC JFET module. It can be seen that the SiC JFET module has much smoother switching characteristics than the Si IGBT module.

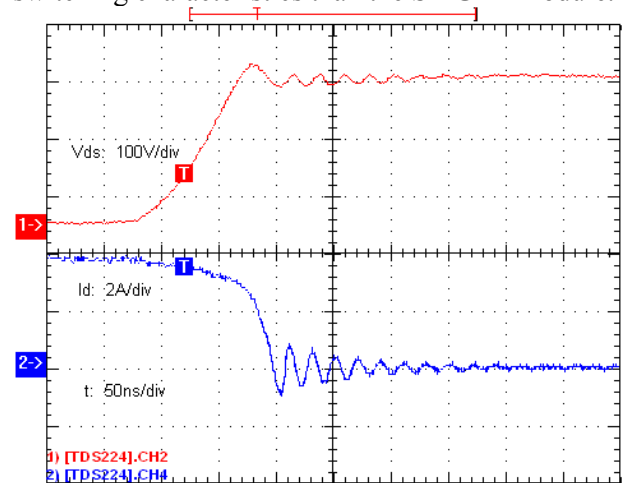


Fig. 27 SiC JFET module turn-off waveforms

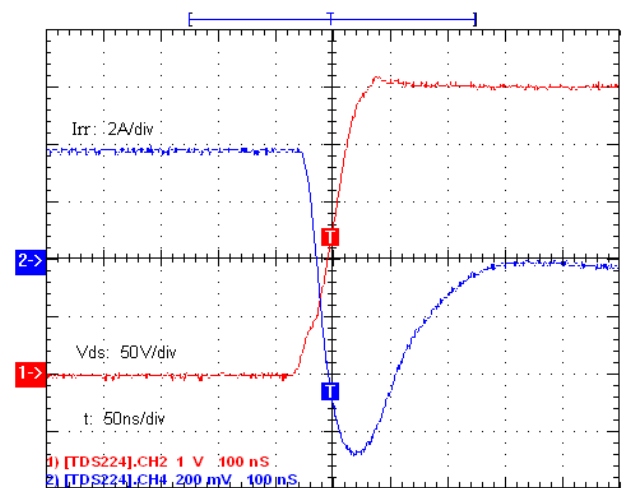


Fig. 28 Si IGBT module reverse current I_{rr}

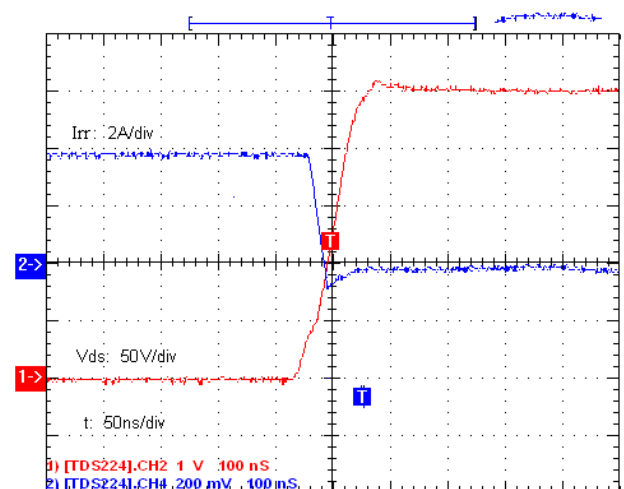


Fig. 29 SiC JFET module reverse current I_{rr}

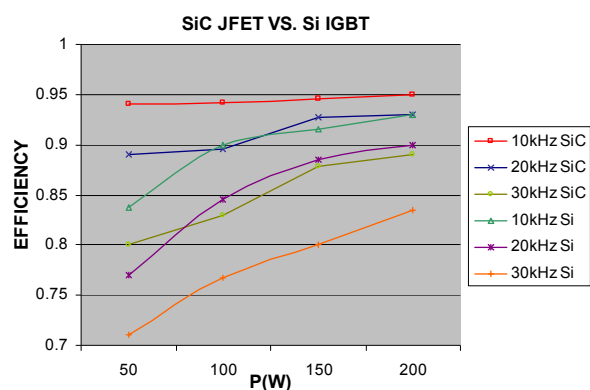


Fig. 30 SiC JFET vs. Si IGBT Inverter efficiency

Fig. 30 shows the experimental efficiency of SiC JFET module based inverter and the 3rd generation Si IGBT module based inverter. The SiC JFET inverter shows 94% efficiency at 20kHz switching frequency at 200W, 150VDC operation, while the Si IGBT-based inverter only achieved 90% efficiency at the same switching frequency. Higher the switching frequency is, Bigger the efficiency gap between SiC JFET inverter and Si IGBT inverter achieves.

4 Conclusion

This paper discussed the design and experiments of SiC JFET based inverter, with special focus on the gate drive circuit design. In this design, the DC rail voltage is used to power the gate drive circuit and to interlock the relay (soft-start) that prevents the power-up of the SiC module before negative gating signal is applied at the gates. The combination of negative gate voltage and the interlock mechanism will prevent the breakthrough of SiC JFET modules that are normally-on device.

The measurement shows significant reduction in switch-on/off time and on-state resistance in SiC JFET modules as compared to conventional IGBT modules. The simulation and experiments on the 3-phase sinusoidal SiC inverter show significant efficiency improvement over conventional IGBT inverters over a wide range of switching frequencies. Since higher switching frequency can be easily achieved in SiC JFET based inverters, a considerable reduction of the size of passive components in inverters can be also anticipated.

In the next phase of study, high temperature operation up to 300oC has also been demonstrated for SiC modules. the operating temperature of the SiC inverter system will be tested. Higher power rating up to 5kW and later 50kW will be achieved by using parallel connected SiC JFETs.

References:

- [1] Hiromichi Ohashi, Power electronics innovation with next generation advanced power devices, *The 25th International Telecommunications Energy Conference, Proceedings of IEEE-INTELEC*, Oct 19-23, volume 1, 2003, pp. 9-13.
- [2] Jian-Song Chen; Sei-Hyung Ryu; Kornegay, K.T. , A silicon carbide CMOS intelligent gate driver circuit with stable operation over a wide temperature range, *IEEE journal of solid-state circuits*, vol. 34, No.2, 1999, pp. 192-202.
- [3] D. Stephani, Prospects of SiC Power Devices from the State of the Art to Future Trends, *Proceedings of the 45th International Power Electronics Conference*, Nuremberg, May 14-16, 2002, K-2.
- [4] L.Lorenz, H.Mitlehner, Key Power Semiconductor Device Concepts for the Next Decade, *IEEE Industry Applications Conference 37th IAS Annual Meeting*, Pittsburgh, Pennsylvania, USA, October 13-18, vol. 1, 2002, pp. 564 – 569.
- [5] Kelley, R. Mazzola, M.S., SiC JFET gate driver design for use in DC/DC converters, *IEEE Applied Power Electronics Conference and Exposition*, 2006, vol. 1, pp. 179-182.
- [6] Round, S.; Heldwein, M.; Kolar, J.; Hofsjager, I.; Friedrichs, P., A SiC JFET driver for a 5 kW, 150 kHz three-phase PWM converter, *IEEE Industry Applications Conference*, 2005. vol.1, pp. 410 – 416.
- [7] T. McNutt, A. Hefner, A. Mantooth, J. Duliere, D. Berning, R. Singh, Silicon Carbide PiN and Merged PiN- Schottky Power Diode Models Implemented in the Saber Circuit Simulator, *IEEE Transactions on Power Electronics*, vol. 19, no. 3, 2004, pp. 573-581.
- [8] T. McNutt, A. Hefner, A. Mantooth, J. Duliere, D. Berning, R. Singh, Parameter Extraction Sequence for SiC Schottky, Merged PiN Schottky, and PiN Power Diode Models, *IEEE Power Electronics Specialists Conference (PESC)*, Cairns, Australia, 2002, pp. 1269-1276.
- [9] A.S. Kashyap, P.L. Ramavarapu, S. Maganlal, T.R. McNutt, A.B. Lostetter, H.A.Mantooth, Modeling Vertica Channel Junction Field Effect Devices in Silicon Carbide, *IEEE Power Electronics Specialists Conf.(PESC)*, Aachen, Germany, 2004, pp. 3009-3014.
- [10] R. Kraus and H. Jurgen, Status and Trends of Power Semiconductor Device Models for Circuit Simulation, *IEEE Transactions on*

- Power Electronics*, vol.13, no.3, 1998, pp. 452-465.
- [11] Chung, G.Y, Tin, C.C, Williams, J.R, McDonald, K, Chanana, R.K, Weller, R.A, Pantelides, S.T, Feldman, L.C, Holland, O.W, Das, M.K, Palmour, J.W, Improved inversion channel mobility for 4H-SiC MOSFETs following high temperature anneals in nitric oxide, *IEEE Electron Device Letters*, Vol.22, No.4, 2001, pp.176-178.
- [12] Chow, T.P., Tyagi, R., Wide bandgap compound semiconductors for superior high-voltage power devices, *Proceedings of the 5th International Symposium on Power Semiconductor Devices and ICs*, Vol.1, 1993, pp. 84-88.
- [13] S. Yoshida, H. Ishii, A High-Power GaN-Based Field-Effect Transistor for Large-Current Operation, *Physica status solidi*, Vol.188, No.1, 2001, pp.243-246.
- [14] Katsunori Asano, Yoshitaka Sugawara, A unified proposal for characteristic testing methods and figure of merit of 8-kV/3.5-kVA class light-triggered thyristors, *Electrical Engineering in Japan*, Vol.140, No.3, 2002, pp.61-70.
- [15] Yoshida, S., Li, J., Wada, T., Takehara, H., High-power AlGaIn/GaN HFET with lower on-state resistance and higher switching time for an inverter circuit, *IEE Proceedings-Circuits, Devices and Systems*, Vol.151, No.3, 2004, pp.207-210.
- [16] Reinhold Schorner, Peter Friedrichs, Dethard Peters, Dietrich Stephani, Sima Dimitrijevic, Philippe Jamet, Enhanced channel mobility of 4H-SiC metal-oxide-semiconductor transistors fabricated with standard polycrystalline silicon technology and gate-oxide nitridation, *Applied Physics Letters*, Vol.80, 2002, pp.4253.
- [17] Kelley, R.L. Mazzola, M.S. Draper, W.A. Casady, J., Inherently safe DC/DC converter using a normally-on SiC JFET, *IEEE Applied Power Electronics Conference and Exposition*, Vol.3, 2005, pp.1561-1565.
- [18] McNutt, T.; Veliadis, V.; Stewart, E.; Hearne, H.; Reichl, J.; Oda, P.; Van Campen, S.; Ostop, J.; Clarke, C.R., Silicon carbide JFET cascode switch for power conditioning applications, *IEEE Conference on Vehicle Power and Propulsion*, Vol.1, 2005, pp.499-506.
- [19] W.M. S. Mazzola, L. Cheng, J. Casady, D. Seale, V. Bondarenko, R. Kelley, and J. Casady, Scalable SiC Power switches for applications in more electric vehicles, *IEEE Proceeding of the All Electric Combat Vehicle Conference (AEVC)*, Vol.1 2005, pp.256-260.
- [20] Bondarenko, V.; Mazzola, M.S.; Kelley, R.; Cai Wang; Yi Liu; Johnson, W., SiC devices for converter and motor drive applications at extreme temperatures, *IEEE Aerospace Conference*, Vol.1, 2006, pp.6.
- [21] Round, S. Heldwein, M. Kolar, J. Hofsajer, I. Friedrichs, P., A SiC JFET driver for a 5 kW, 150 kHz three-phase PWM converter, *IEEE Industry Applications Conference*, Vol.1, 2005, pp.410-416.
- [22] Zolper, J.C., Emerging silicon carbide power electronics components, *IEEE Applied Power Electronics Conference and Exposition*, 2005 Vol.1, 2005, pp.11-17.
- [23] Wang, Y. Callaway J. Cass Chow, T.P. Wang, F. Boroyevich, D., SPICE Model of SiC JFETs for Circuit Simulations, *IEEE Workshops on Computers in Power Electronics*, Vol.1, 2006, pp.212-215.
- [24] Hernandez-Mora, M., Akuffo, A.; Hood, C., Ortiz-Rodriguez, J.M., Hefner, A., Experimental Evaluation of SiC PiN Diode Forward Bias Degradation and Long Term Stability, *IEEE Power Electronics Specialists Conf (PESC)*, Vol.1 2008, pp.61-65.
- [25] Cheriti, A. Al-Haddad, K. Mukhedkar, D., Calculation of power loss in soft commutated PWM inverters, *IEEE Industry Applications Society Annual Meeting*, 1991, vol. 1, pp. 782-788.
- [26] Schafmeister, F. Herold, S. Kolar, J.W., Evaluation of 1200 V-Si-IGBTs and 1300 V-SiC-JFETs for application in three-phase very sparse matrix AC-AC converter systems, *IEEE Applied Power Electronics Conference and Exposition*, Vol.1, 2003, pp.241-255.
- [27] Hua Bai, Sanbo Pan, Chris Mi, Sonya Gargies, Tim Lin. " A Functional Model of Silicon Carbide JFET and Its Use in the Analysis of Switching-Transient and Impact of Gate Resistor, Miller Effect, and Parasitic Inductance" , *International Journal of Power Electronics* , Vol2, No.2,2010, pp.164-175.
- [28] Sanbo Pan, Chris Mi, Tim Lin, " Design and Testing of Silicon Carbide JFETs Based Inverter " , *IEEE 6th International Power Electronics and Motion Control Conference (IPEMC 2009)*, 2009, pp.2556-2560.